ELSEVIER

Chemical Engineering Journal 135S (2008) S159–S165

Chemical Engineering Journal

www.elsevier.com/locate/cej

Velocity fluctuations of segmented flow in microchannels

V. van Steijn [a,*], M.T. Kreutzer [b], C.R. Kleijn [a]

[a] *Delft University of Technology, Faculty of Applied Sciences, Department of Multi-Scale Physics, Prins Bernhardlaan 6, 2628 BW, Delft, The Netherlands*
[b] *Delft University of Technology, Faculty of Applied Sciences, DelftChemTech, Julianalaan 136, 2628 BL, Delft, The Netherlands*

Abstract

This paper describes the velocity fluctuations of segmented gas–liquid flow in a microfluidic channel. The fluctuations are caused by pressure fluctuations associated with bubble formation and bubbles leaving the channel. Instantaneous bubble velocities were measured with a high speed camera at different locations in the channel. The observed transients could be decomposed into contributions of the pump, the inlet and the outlet. Experiments were performed for different velocities and bubble and slug lengths. A simple scaling analysis successfully predicted the order of magnitude of these fluctuations.

Keywords: Taylor flow; Instability; Transients; Gas–liquid flow; Outlet effect; Bubble; Droplet

1. Introduction

Segmented multiphase flows in microchannels [1–5] are dominated by interfacial stresses [6]: the pressure inside the elongated bubbles is higher by an amount $\Delta p \sim \gamma/d$, where γ is the interfacial tension and d is the bubble diameter. As a result, the pressure drop over a not-too-long channel changes significantly by the creation or destruction of a single gas–liquid interface. The movement of bubbles through microfluidic channels then resembles a rowing boat, in the sense that it decelerates and accelerates with a regular period. This period corresponds to the period between bubbles entering and/or leaving the channel. These pressure fluctuations, and the flow fluctuations they induce, are the subject of this paper.

Notwithstanding these pressure fluctuations and their resulting stability problems, adding a gas phase can dramatically improve micromixing [7] as well as the conversion levels and obtained selectivities in chemical reactions and material synthesis, even if no gas is required for the reaction to proceed. The benefits of segmented flow in chemical reactions and material synthesis include the following:

- The recirculation in the slugs enhances micromixing [8,9], compared to the slow purely diffusive micromixing in single-phase flow [10].
  This is especially relevant when the micromixing time must be fast enough to avoid unwanted side reactions.
- Only a thin lubricating liquid film connects subsequent liquid slugs, and reagent carry-over from slug to slug is very small. This reduces the wash-time between subsequent reagents in high-throughput applications [11,12].
- When the walls of the microchannel are functionalized, e.g. with a biological assay or a heterogeneous catalyst, the mass transfer of reagents is dramatically enhanced [13].

The characteristic times underlying the above-described phenomena are all strong functions of the characteristic bubble velocity U_b or the thickness of the lubricating film d_{film}, which in turn is determined by U_b and fluid properties [14]. Günther et al. [9] demonstrated that the micromixing time t_{mix} is mostly determined by the Peclet number $Pe = U_b x/D$. Sample carry-over depends on the time $t_{film} = d_{film}^2/D$ required to penetrate significantly into the lubricating film. The mass transfer rate to the wall can, to leading order, be estimated using film theory as $k_m = D/d_{film}$ [13]. So, fluctuations in the bubble velocity U_b should be avoided when one investigates reacting segmented flows. Additionally, fluctuations in bubble velocity should be avoided in measurements of the flow field, where U_b is either subtracted from measured values or where the channel translates with a velocity U_b to keep the bubble in the field of view.

The most common oscillatory slug flow occurs in pulsating heat pipes, where flow transients are induced by boiling (e.g. [15]). In contrast to such forced oscillations, where the

* Corresponding author.
E-mail address: V.vanSteijn@tudelft.nl (V. van Steijn).

1385-8947/$ – see front matter © 2007 Elsevier B.V. All rights reserved.
doi:10.1016/j.cej.2007.07.037

Nomenclature

d	diameter (m)
d_{film}	thickness of the lubricating film (m)
D	diffusion coeffient (m^2/s)
k	hydraulic coefficient
k_m	mass transfer coefficient (m/s)
L	length (m)
n	number of bubbles in the channel
p	pressure (Pa)
Δp	pressure drop over the channel (Pa)
$\Delta(\Delta p)$	variations in pressure drop (Pa)
t	time (s)
t_{film}	diffusion time (s)
t_{mix}	micromixing time (s)
U	velocity (m/s)
$\Delta(U_b)$	variations in bubble velocity (m/s)
x	distance from T-junction (m)

Greek letters

γ	surface tension (N/m)
μ	viscosity (Pa s)
ρ	density (kg/m^3)
σ	standard deviation

Dimensionless numbers

τ	dimensionless time, $\tau = tU_b/(L_b + L_s)$
Ca	Capillary number, $Ca = \mu_l U_b/\gamma$
Pe	Peclet number, $Pe = U_b x/D$

Subscripts

b	bubble
ch	channel
f	front
g	gas
i	internal
l	liquid
r	rear
s	slug
tot	total

frequency depends on the heating rate, we focus in this work on oscillations induced by the flow itself. Pioneering work on velocity fluctuations under isothermal conditions by Reinecke and Mewes [16] showed that the compressibility of the gas in the gas-feed line leads to significant transients with long periods of oscillation. Their work demonstrated that the flow fluctuations can be significantly reduced by minimizing the volume of the gas-feed channel. In practice, creating a huge pressure drop in the gas-feed line, relative to the pressure drop in the multiphase flow downstream, has the same effect. For this reason, the use of gas-feed lines of very small diameter is now common practice in multiphase microfluidics.

The work of Reinecke and Mewes [16] balanced the pressure in the gas-feed with the pressure drop inside the channel, and ignored pressure terms due to gas–liquid interfaces in the microchannels. Chio et al. [17] recently described the pressure pulse associated with the flow of a bubble through a contraction in a microchannel. The change in curvature was the dominant contribution to this pulse. Such a pressure pulse affects the motion of elongated bubbles in a segmented gas–liquid flow and even can have an effect on the formation process as reported by Salman et al. [18]. We have found in our work that the flow of bubbles through such contractions, perhaps in the form of a fluidic connection to a chip, can cause significant flow fluctuations. Similarly, we found that the pressure pulses caused by bubble leaving the channel can cause velocity variations of more than 30% of the mean velocity.

The paper is organized as follows. We first describe our experiments and the raw data of velocity fluctuations. Subsequently, we describe experiments to determine whether these fluctuations predominantly occur at the outlet or the inlet, and how the fluctuations change with location in the channel. Finally, we present a scaling analysis that estimates the amplitude of bubble velocity variations, caused by bubble generation and destruction.

2. Experimental

2.1. Microfluidic device

The microfluidic device (Fig. 1) was fabricated in a flat plate of polymethyl methacrylate (PMMA) by precision milling and sealed by a thin PMMA cover slide, where chloroform was used to bond both pieces. Stainless steel round auxiliary channels were connected to both the gas inlet ($d_i = 254\,\mu m$, $L = 4$ m) and the liquid inlet ($d_i = 0.5$ mm, $L = 37$ cm) and were glued in place with epoxy. The dimensions of these channels were chosen such that the pressure drop over the auxiliary channels was approximately one order of magnitude larger compared to the pressure drop in the segmented flow section [19]. In this way, pressure fluctuations in the segmented flow section will not affect the inflow of gas and liquid. The outflow was allowed to vent to the atmosphere.

The gas and liquid stream, introduced from separate inlets, were mixed in a T-junction (Fig. 1), which is located nearly 50 channel diameters, d_{ch}, downstream of the liquid inlet to

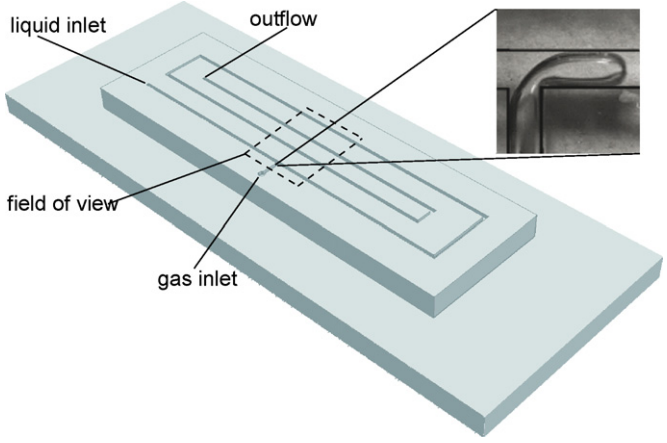

Fig. 1. Microfluidic device.

ensure a fully developed liquid flow. Over the entire length of the device ($L = 317$ mm, $L/d_{ch} \approx 396$), the square cross-section equals 0.8 mm × 0.8 mm. Gas was supplied from a pressurized vessel and controlled by a flow controller (porter, vcd-1000), while liquid was delivered from a 60 mL syringe by a syringe pump (KD Scientific, KDS 210). The working fluids were ethanol ($\rho_l = 789$ kg/m^3, $\mu_l = 1.201 \times 10^{-3}$ Pa s) and air ($\rho_g = 1.205$ kg/m^3, $\mu_g = 1.82 \times 10^{-5}$ Pa s), with a surface tension of $\gamma = 22.8 \times 10^{-3}$ N/m. This system can be considered as hydrophilic, since good wetting of ethanol over the PMMA surface was observed. All experiments were conducted at ambient pressure and room temperature. The temperature was accurately recorded and in the post-processing of the data, the influence of temperature on the fluid properties was accounted for.

2.2. High speed camera set-up

The motion of elongated bubbles was studied using a high speed camera (Olympus, i-SPEED). The field of view (see Fig. 1) was set-up such that one image contained multiple bubbles, while still having high enough spatial resolution to resolve the edges of the bubbles accurately. The field of view included the T-junction where the gas- and liquid-feed meet. The instances of bubble formation at this T-junction were recorded. The images were evaluated as follows. First, the images were binarized using thresholding. Second, the positions of the front, $x_f(t)$, and rear, $x_r(t)$, of the bubbles were tracked in time. The displacement of a bubble from frame to frame was approximately 4 pixels. Third – before calculating the velocity by taking the time derivative of $x_f(t)$ and $x_r(t)$ – the data was smoothened by fitting a third-order polynomial through 7 points centered around the point under consideration. In this way, velocity data was obtained for each individual front and rear. The velocity data obtained for the front and rear of a bubble were in close agreement, and we calculated the bubble velocity by averaging the velocity of the front and the rear of the bubble. Three bubbles could be tracked at every point in time. The instantaneous velocities of each of these three bubbles were in sync at all times, and these three velocities were averaged to finally obtain the evolution of velocity in time. The use of the polynomial fit and the averaging allowed us to obtain sub-pixel resolution for the displacement. As the flow rates were varied, the lengths of the bubbles and slugs varied as well. The lengths of at least 8 bubbles and slugs were measured from the recorded images, and the average bubble and slug length was recorded. In all experiments, we obtained a very regular flow pattern, and the variation of bubble and slug length was within 2%.

3. Results and discussion

3.1. Experimental observations

Fig. 2 shows how the bubble velocity varies with time for several gas flow rates and liquid flow rates. We studied the fluctuations in bubble velocity for different velocities and different bubble and slug lengths, which are presented in the left and right column, respectively. We normalized the time with respect to the period in which a full bubble and a full slug passed an arbitrary cross-section of the channel, i.e. $\tau = tU_b/(L_b + L_s)$. This period coincides with the period between two bubble formations at the T-junction; the vertical grid lines in Fig. 2 indicate the moment that a bubble formed at the inlet T-junction. In most cases, the bubble velocity fluctuated around its mean value by ∼10–30%. In some cases, most notably for long bubbles and short slugs, the bubbles came to a short but complete stop.

From Fig. 2, four main observations can be made.

- The three images on the left show that, when the bubble length and slug length are kept constant and the velocity increases, the relative fluctuations decrease with increasing flow rate.
- The three images on the right show that, at fixed bubble velocity, the relative fluctuations increase for increasing bubble to slug length ratio.
- The fluctuations exhibit a clear periodicity, with a period similar to that of bubble generation.
- The large dips in velocity observed in the right column for cases with long bubbles and short slugs and leading to a complete stop of the bubbles, correlate well with the moment that a bubble forms at the T-junction, while no peaks could be attributed to the bubble formation for the cases presented in the left column.

All these observations are consistent with our postulate that the velocity fluctuations are resulting from pressure fluctuations due to the creation and destruction of bubbles, as will be demonstrated in the next section.

We measured the variation of velocity due to the syringe pump by trapping a single bubble in the channel and measuring its velocity. The standard deviation of the velocity of this single bubble was 2%, due to irregularities in the syringe screw.

In order to determine the relative contributions of the inlet and the outlet on the fluctuations, we performed the following so-called startup experiment. First, the channel was filled with liquid and the liquid pump was started. When a stable liquid flow had formed, the gas flow was switched on, and bubbles started to appear in the channel. As these first bubbles flowed through the channel, we recorded their velocities. Until the bubbles reach the exit of the channel, all fluctuations that occur must be attributed to inlet effects and fluctuations of the pump flow rate. Another possibility would be an influence due to the sharp bends in the channel. However, no significant increase or decrease of velocity fluctuations was observed as, in the startup experiments, the bubbles started to pass through bends. On the other hand, as the bubbles started to leave the channel, the fluctuations increased significantly, as can be seen in Fig. 3. The top part of Fig. 3 shows several periods of velocity measurements. For each period, we calculated the standard deviation of the bubble velocity, $\sigma(U_b)$, and this is plotted in the bottom half of the figure.

After two to three bubbles left the channel, $\sigma(U_b)$ reached a constant steady-state level. From the difference in the steady-state value and the initial values, we estimated all contributions. Before bubbles leave the channel, $\sigma(U_b) \approx 0.03U_b$, which is just

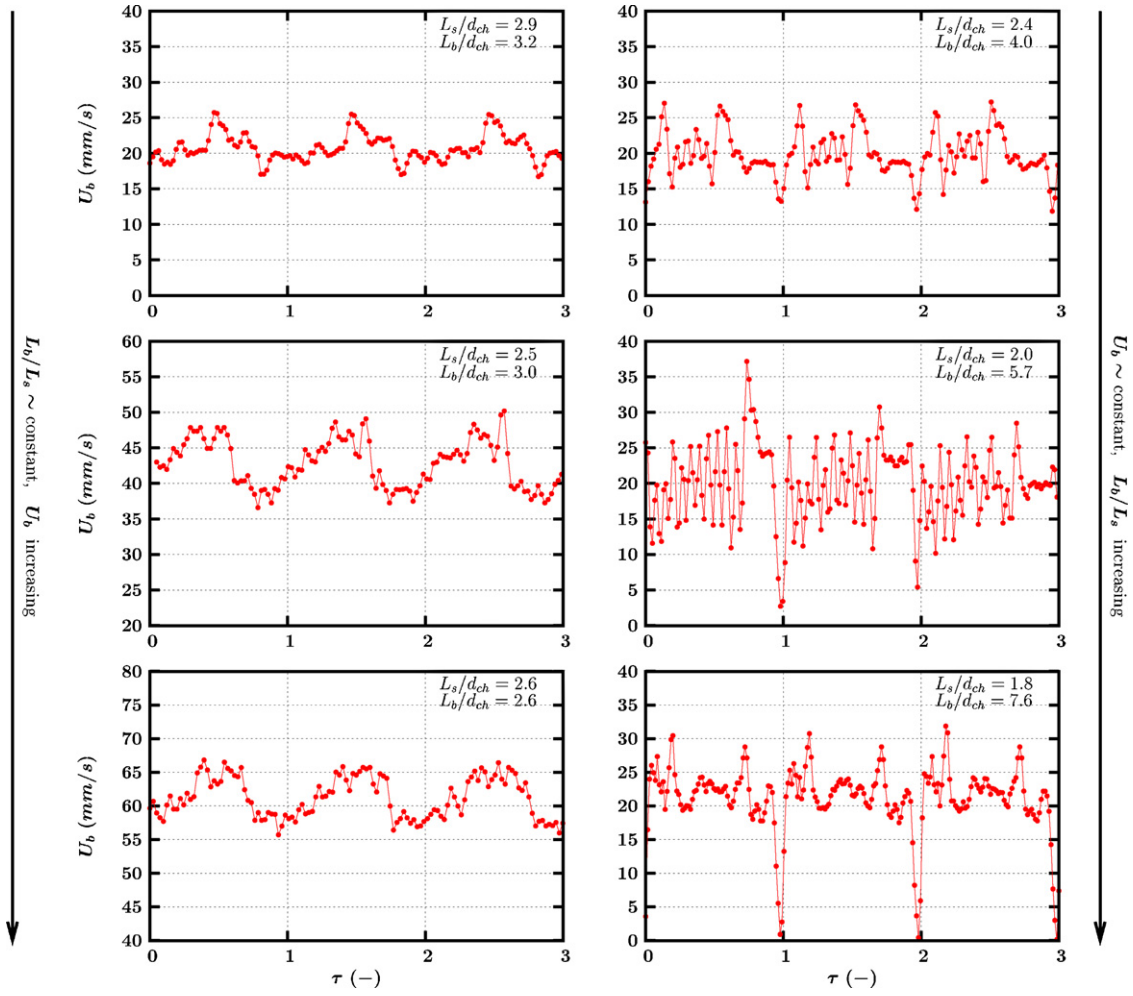

Fig. 2. Bubble velocity as a function of dimensionless time, τ in case of *Left*: approximately constant gas hold up and increasing velocity and *Right*: approximately constant velocity, increasing gas holdup.

above the value of $0.02U_b$ that we had earlier attributed to the pump. So, apparently the inlet does not cause significant variations in flow. The steady-state level, however, is significantly higher, $0.1U_b$, and we conclude that for the experimental conditions in Fig. 3, the exit caused most of the observed transients.

After a long time of steady-state operation, the gas flow was shut down. This caused a sudden fall in bubble velocity. Also, no new bubbles were created and all fluctuations are due to the exit and the pump. The right-hand part of Fig. 3 shows that the fluctuations slowly die out as more bubbles leave the system and the channel becomes fully liquid-filled again.

We studied the bubble velocities simultaneously at three different locations in the channel. These segments were located in the second, third and fourth branch of the channel (see Fig. 1), at $x/d_{ch} \sim 116$, $x/d_{ch} \sim 226$ and $x/d_{ch} \sim 305$, respectively, where x is the distance from the T-junction. In Fig. 4, the relative velocity fluctuations are shown for the three segments in case of a comparable bubble and slug length and mean velocity of 20.7 mm/s. The largest fluctuations were observed near the outflow and the amplitude of the fluctuations dampens out with increasing distance from the outflow for the case shown in Fig. 4. If we extrapolate the dampening linearly to the T-junction, then the amplitude of the fluctuations at the T-junction is only slightly larger than the fluctuations induced by the pump, and agrees nicely with the fluctuations we observed during a startup experiment. Since in many applications mixing occurs mostly at the inlet section, where velocity fluctuations due to outlet effects are relatively small and can be overcome by using a sufficiently long channel, the results suggest that for such applications it is more important to focus on stable pump flow than on outlet effects.

3.2. Scaling analysis and order of magnitude estimation of the fluctuations

The aim of this section is to present a scaling analysis that enables us to predict the order of magnitude of the velocity fluctuations due to bubbles escaping at the outlet and bubble creation at the inlet and their dependence on various flow parameters. We start by describing the relative pressure fluctuations and transform those into velocity fluctuations later on. The pressure fluctuations, $\Delta(\Delta p)$, are compared with the total pressure drop over the segmented-flow section, $(\Delta p)_{tot}$, which can be described as the sum of the pressure drop over the liquid phase, $(\Delta p)_l$, and gas phase, $(\Delta p)_g$.

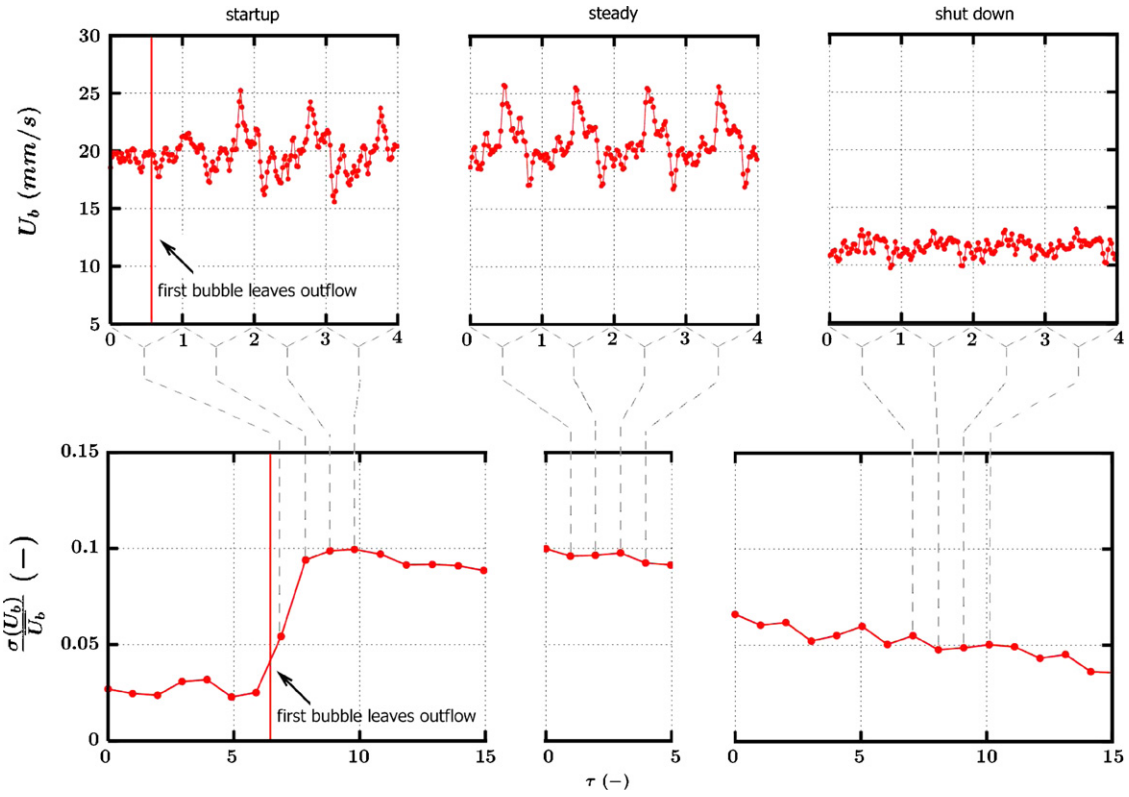

Fig. 3. *Top*: bubble velocity, U_b, and *Bottom*: velocity fluctuations characterized by $\sigma(U_b)/U_b$, both as a function of normalized time τ in case of start-up, steady operation and shutdown for $L_s \sim L_b$.

The pressure drop over the liquid phase, described by the Hagen–Poiseulle equation for laminar flow, is

$$(\Delta p)_l = n\frac{k}{2}\left(\frac{\mu_l U_b}{d_{ch}}\right)\left(\frac{L_s}{d_{ch}}\right) \quad (1)$$

with μ_l is the liquid viscosity, d_{ch} the channel diameter, n the number of bubbles, and L_s is the slug length. The coefficient k equals 56.91 for channels of square cross-section.

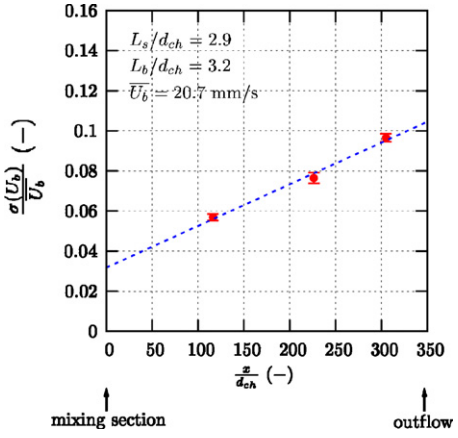

Fig. 4. Relative velocity fluctuations as a function of the distance from the mixing section.

According to Bretherton [14], the pressure losses over the gas phase can be written as

$$(\Delta p)_g = nC(3Ca)^{2/3}\left(\frac{\gamma}{d_{ch}}\right) \quad (2)$$

with Ca is the capillary number. For simplicity, we used the channel diameter instead of the bubble diameter, since both are of nearly the same size. Using a lubrication analysis, Bretherton [14] found a value of $C = 7.16$ for round capillaries. Wong et al. [20] found C in square channels to be one third of that in round channels. Therefore, a value of $C = 2.39$ is used throughout this paper.

Hence, the total pressure drop over the segmented flow section can be written as

$$(\Delta p)_{tot} = n\left(\frac{\mu_l U_b}{d_{ch}}\right)\left[\frac{k}{2}\left(\frac{L_s}{d_{ch}}\right) + C(3)^{2/3}(Ca)^{-1/3}\right] \quad (3)$$

where, for the cases studied in this paper, both contributions were of the same order of magnitude.

The pressure jumps across the rear or front of an elongated bubble, $\Delta(\Delta p)$, are of the order γ/d_{ch}.

The relative pressure fluctuations can then be written as

$$\frac{\Delta(\Delta p)}{(\Delta p)_{tot}} = \frac{\gamma}{nU_b\mu_l[(k/2)(L_s/d_{ch}) + C3^{2/3}(\gamma/U_b\mu_l)^{1/3}]} \quad (4)$$

Note that, for fixed L_s/d_{ch}, these relative fluctuations are independent of channel diameter. Furthermore, the relative fluc-

tuations decrease linearly with the number of bubbles present in the channel.

The fluctuations in pressure drop propagate into velocity fluctuations as

$$\frac{\Delta(U_b)}{U_b} = \frac{1}{U_b}\left(\frac{\partial(\Delta p)_{tot}}{\partial U_b}\right)^{-1}\Delta(\Delta p) \quad (5)$$

The partial derivative $(\partial(\Delta p)_{tot}/\partial U_b)$ is obtained from Eq. (3) and combined with Eq. (4) for $\Delta(\Delta p)$. This leads to

$$\frac{\Delta(U_b)}{U_b} = \frac{\gamma}{\mu_l U_b n[(k/2)(L_s/d_{ch}) + (2/3)C3^{2/3}(\gamma/\mu_l U_b)^{1/3}]} = \frac{(Ca)^{-1}}{n[(k/2)(L_s/d_{ch}) + (2/3)C3^{2/3}(Ca)^{-1/3}]} \quad (6)$$

This equation predicts the maximum deviations in velocity, $\Delta(U_b)$. Throughout this paper, we have used the standard deviation $\sigma(U_b)$ as described in Fig. 3 as a measure for the variation in velocity. We expect that the standard deviation is smaller than the maximum deviation, $\sigma(U_b) < \Delta(U_b)$, even if inlet and outlet effects both contribute to the transients. Still, the two measures will be of the same order and scale similarly with the parameters in Eq. (6).

Fig. 5 plots the right-hand side of Eq. (6) versus $\sigma(U_b)/U_b$ for a wide range of operating conditions ($0.01\,m/s < U_b < 0.07\,m/s$, $38 < n < 70$ and $0.4 < L_b/L_s < 4$), measured under steady-state, close to the exit at $x/d_{ch} = 305$. The figure shows that the standard deviation was always smaller than the predicted maximum deviation, as expected. The data also shows that the scaling analysis is successful in predicting the order of magnitude of the velocity fluctuations for the studied range of operating conditions, as well as the scaling behaviour of its maximum value.

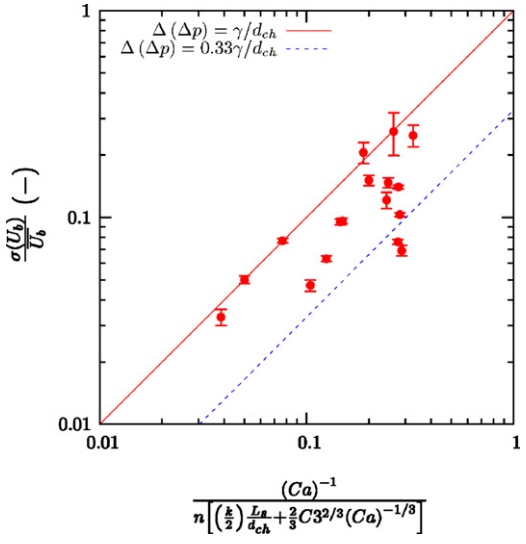

Fig. 5. Relative velocity fluctuations as a function of the relative pressure fluctuations. The solid line indicates parity for Eq. (6). The dotted line indicates fluctuations of one third of those predicted by Eq. (6). For each experiment, $\sigma(U_b)$ was determined over eight periods, and the error bars indicate the variation from period to period.

3.3. Discussion and practical implications

In most engineering applications, one would like to avoid velocity fluctuations, as mentioned in the introduction. The analysis presented in Eq. (6) and Fig. 5 provides quantitative engineering guidelines how to keep the fluctuations below a desired limit. For given fluid properties (γ, μ_l), dictated by the application at hand, the obvious way to reduce the relative velocity fluctuations is to increase the number of bubbles n (that is to increase the length of the channel) or to increase the bubble velocity U_b. For a prescribed residence time, this should be done at fixed n/U_b. If one has some degree of freedom in choosing the liquid, a high liquid viscosity μ_l and low surface tension γ are to be preferred. For a given geometry, k and C are fixed constants and changing the geometry only has a moderate impact on these constants.

We have shown in this paper that the observed velocity fluctuations are predominantly due to the pressure burst of order γ/d when a bubble leaves the channel. It is therefore to be expected that variations in the outlet geometry, for instance a smoothly increasing cross-section d, will lead to reduced pressure fluctuations. Since the layout of most microfluidic devices has limited flexibility in the depth dimension, such expansion is most easily achieved by ejecting the bubble intact from the chip and by expanding the exit tube.

4. Conclusions

In this article, the fluctuations in the velocity of gas bubbles traveling through a microfluidic device, operated in segmented gas–liquid flow, were described. By using a high speed camera, we were able to determine the instantaneous bubble velocities and fluctuations therein.

- The observed transients were found to be due to pressure fluctuations, which were decomposed into contributions from the pump, from the inlet and from the outlet.
- In our set-up, the contribution from the outlet was dominant under most conditions.
- For long bubbles, phenomena at the inlet were also important.
- The velocity fluctuations were strongest near the outlet, although the fluctuations extend very far into the channel and seem to decay only linearly with distance from the outlet.
- The experimental results were in good agreement with a simple theoretical model, which describes the relation between the relative velocity fluctuations and relative pressure drop fluctuations.

Acknowledgements

This work was supported by the Delft Centre for Sustainable Industrial Processes (DCSIP). M.T.K. is supported by a VENI grant from NWO chemical sciences.

References

[1] A. Günther, S.A. Khan, M. Thalmann, F. Trachsel, K.F. Jensen, Transport and reaction in microscale segmented gas–liquid flow, Lab Chip 4 (2004) 278–286.

[2] M.T. Kreutzer, F. Kapteijn, J.A. Moulijn, J.J. Heiszwolf, Multiphase monolith reactors: chemical reaction engineering of segmented flow in microchannels, Chem. Eng. Sci. 60 (2005) 5895–5916.

[3] M.T. Kreutzer, F. Kapteijn, J.A. Moulijn, C.R. Kleijn, J.J. Heiszwolf, Inertial and interfacial effects on pressure drop of Taylor flow in capillaries, AIChE J. 51 (2005) 2428–2440.

[4] V.S. Ajaev, G.M. Homsy, Modeling shapes and dynamics of confined bubbles, Annu. Rev. Fluid Mech. 38 (2006) 277–307.

[5] H.A. Stone, A.D. Stroock, A. Ajdari, Engineering flows in small devices: Microfluidics toward a lab-on-a-chip, Annu. Rev. Fluid Mech. 36 (2004) 381–411.

[6] P.-G. de Gennes, F. Brochard-Wyart, D. Quéré, Capillarity and Wetting Phenomena: Drops, Pearls, Waves, Springer, New York, 2003.

[7] P. Garstecki, M.J. Fuerstman, M.A. Fischbach, S.K. Sia, G.M. Whitesides, Mixing with bubbles: a practical technology for use with portable microfluidic devices, Lab Chip 6 (2006) 207–212.

[8] H. Song, M.R. Bringer, J.D. Tice, C.J. Gerdts, R.F. Ismagilov, Experimental test of scaling of mixing by chaotic advection in droplets moving through microfluidic channels, Appl. Phys. Lett. 83 (2003) 4664–4666.

[9] A. Günther, M. Jhunjhunwala, M. Thalmann, M.A. Schmidt, K.F. Jensen, Micromixing of miscible liquids in segmented gas–liquid flow, Langmuir 21 (2005) 1547–1555.

[10] P.J.A. Kenis, R.F. Ismagilov, G.M. Whitesides, Microfabrication inside capillaries using multiphase laminar flow patterning, Science 285 (1999) 83–85.

[11] T.C. Thulasidas, M.A. Abraham, R.L. Cerro, Dispersion during bubble-train flow in capillaries, Chem. Eng. Sci. 54 (1) (1999) 61–76.

[12] R.E. Thiers, A.H. Reed, K. Delander, Origin of the lag phase of continuous-flow analyis curves, Clin. Chem. 17 (1) (1971) 42–48.

[13] M.T. Kreutzer, P. Du, J.J. Heiszwolf, F. Kapteijn, J.A. Moulijn, Mass transfer characteristics of three-phase monolith reactors, Chem. Eng. Sci. 56 (2001) 6015–6023.

[14] F.P. Bretherton, The motion of long bubbles in tubes, J. Fluid Mech. 10 (1961) 166–188.

[15] S.B. Liang, H.B. Ma, Oscillating motions of slug flow in capillary tubes, Int. Commun. Heat Mass Transfer 31 (2004) 365–375.

[16] N. Reinecke, D. Mewes, Oscillatory transient two-phase flows in single channels with reference to monolithic catalyst support, Int. J. Multiphase Flow 25 (1999) 1373–1393.

[17] H. Chio, M.J. Jensen, X. Wang, H. Bruus, D. Attinger, Transient pressure drops of gas bubbles passing through liquid-filled microchannel contractions: an experimental study, J. Micromech. Microeng. 16 (2006) 143–149.

[18] W. Salman, A. Gavriilidis, P. Angeli, On the formation of Taylor bubbles in small tubes, Chem. Eng. Sci. 61 (2006) 6653–6666.

[19] N. de Mas, A. Günther, T. Kraus, M.A. Schmidt, K.F. Jensen, Scaled-out multilayer gas–liquid microreactor with integrated velocimetry sensors, Ind. Eng. Chem. Res. 44 (2005) 8997–9013.

[20] H. Wong, C.J. Radke, S. Morris, The motion of long bubbles in polygonal capillaries. part 2. Drag, fluid pressure and fluid flow, J. Fluid Mech. 292 (1995) 95–110.